RSC Advances

PAPER

View Article Online
View Journal | View Issue

Cite this: *RSC Adv.*, 2020, **10**, 9717

Histidine-conjugated DNA as a biomolecular depot for metal ions†

Soyoung Park, *[a] Haruka Matsui,[a] Koyuki Fukumoto,[a] Ji Hye Yum[a] and Hiroshi Sugiyama *[ab]

Received 10th February 2020
Accepted 26th February 2020

DOI: 10.1039/d0ra01267j

rsc.li/rsc-advances

Histidine is a versatile amino acid residue that plays a critical role in the active sites of many metalloenzymes. DNA is an attractive biomolecular scaffold owing to its chemical and thermal stability and easy accessibility. Herein, we report histidine-conjugated DNA oligonucleotides, which were synthesized by combining DNA alphabets and natural metal-binding amino acids, as novel biohybrid materials and demonstrate their use as molecular depots for various metal ions. Moreover, histidine-conjugated DNA oligonucleotides could be successfully used in asymmetric catalysis (up to 90% conversion and 95% *ee*) as DNA metalloenzymes and in 2,2′-azino-bis(3-ethylbenzothiazoline-6-sulfonic acid) oxidation reactions as horseradish-peroxidase (HRP)-mimicking DNAzymes with suitable metal cofactors. Nature-inspired histidine-DNA hybrids will become an attractive strategy to construct fine-tuned coordination environments as an alternative to bioremediation and the development of multimetal enzymes.

Introduction

Nucleic acids, especially DNA, are useful biomolecules to develop molecular engineering materials for various applications in chemical biology and biomedicine. They have many advantages including straightforward automated synthesis processes, unique complementarity, and high selectivity and affinity for target biomolecules such as proteins.[1–4] DNA has been actively explored as a versatile building block in nanotechnology owing to its superior, programmable self-assembling abilities and the high rigidity of its secondary structures.[5–7] In addition, DNA is highly amenable to structural modification and introduction of functional groups. The applications of DNA can be further enhanced by the introduction of various functional groups such as fluorescent dyes,[8–10] alkylating agents,[11–13] and metal-binding ligands.[14–16] Among them, site-specific functionalization of DNA with metal ions has received attention because of the wide range of its applications, including molecular magnets,[17–19] electron transport chains,[20–22] and metalloenzymes.[23–26] Several metal-mediated natural or artificial nucleobase pairs have been explored and various metal-binding ligands, such as bipyridine (bpy) and terpyridine, have been used in the development of metal-modified DNA.[27–29]

In our previous study, we established the covalent anchoring strategy for direct incorporation of intrastrand metal-binding ligands such as bpy into the DNA phosphate backbone.[24,30–32] We generated a series of Cu (bpy)-containing DNA hybrid catalysts and achieved asymmetric intramolecular Friedel–Crafts alkylation[28] and enantioselective hydration reactions.[33] We also interspersed a bpy ligand into the DNA strands using an acyclic D-threoninol backbone, which is a versatile moiety for the modification of oligonucleotides with carboxylic acid derivatives.[33] In this study, we focused on histidine (**His**), an amino acid residue that plays a critical role in the active sites of many metalloenzymes. Because the imidazole ring of histidyl peptide residues provides an excellent coordination environment for various metal ions, imidazole-modified oligonucleotides have been investigated. Müller and colleagues synthesized a DNA oligonucleotide containing three consecutive imidazole ligands and reported the nuclear magnetic resonance solution structure of metal-modified DNA with imidazole–Ag(I)-imidazole base pairs.[34–36] Recently, Clever and colleagues reported on imidazole-modified G-quadruplex DNA.[37,38] They incorporated an imidazole ligand into DNA using a glycidol linker and demonstrated a potential Cu(II)-sensory application involving the peroxidase-mimicking DNAzyme activity of this complex. Surprisingly, to our knowledge, the direct incorporation of **His** residues into DNA oligonucleotides has not yet been reported. Herein, we report the synthesis and characterization of **His**-conjugated DNA oligonucleotides with a distinctive metal-binding ability. Furthermore, **His**-conjugated DNA oligonucleotides could be successfully used in asymmetric catalysis as well as 2,2′-azino-bis(3-ethylbenzothiazoline-6-sulfonic acid) (ABTS) oxidations in the presence of suitable metal cofactors.

[a]*Department of Chemistry, Graduate School of Science, Kyoto University, Kitashirakawa-oiwakecho, Sakyo-ku, Kyoto 606-8502, Japan. E-mail: hs@kuchem.kyoto-u.ac.jp; oleesy@kuchem.kyoto-u.ac.jp*

[b]*Institute for Integrated Cell-Material Sciences (iCeMS), Kyoto University, Yoshida-ushinomiyacho, Sakyo-ku, Kyoto 606-8501, Japan*

† Electronic supplementary information (ESI) available: Details of the material, compound synthesis, catalytic reactions, and molecular modeling information. See DOI: 10.1039/d0ra01267j

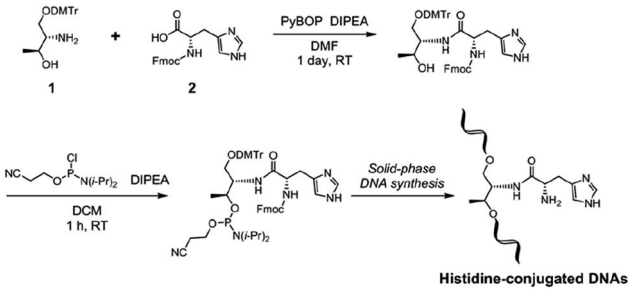

Scheme 1 Synthesis of histidine-conjugated DNA oligonucleotides.

Results and discussion

A synthetic route for **His**-conjugated oligodeoxynucleotides is shown in Scheme 1.

Acyclic D-threoninol is a versatile backbone for the modification of DNA, and acyclic threoninol nucleic acids (*a*TNA) have been well investigated by Asanuma and colleagues.[39–41] We have also established a DNA modification approach using the threoninol moiety to incorporate a bpy ligand into the DNA oligonucleotide strands for the synthesis of bpy-containing DNA hybrid catalysts.[33] For incorporation of **His** into oligonucleotides, it is important to select an appropriate amino-protecting group for the **His** residue that is able to tolerate not only phosphitylation conditions but also the solid-phase DNA synthesis process. In this study, we used fluorenylmethoxycarbonyl (Fmoc)-protected **His**. The Fmoc group is compatible with the chemical reagents used during phosphitylation and solid-phase oligonucleotide synthesis. In addition, removal of the Fmoc group could be accomplished during standard cleavage and deprotection conditions using an aqueous solution of methylamine and ammonium hydroxide. Regarding the imidazole group of **His**, an unprotected imidazole group could be incorporated into DNA oligonucleotides. Based on previous studies,[24,28,33] DMTr-protected D-threoninol (**1**) could be conjugated with Fmoc-protected **His** (Fmoc–**His**–OH, **2**) in the presence of PyBOP and DIPEA. After phosphitylation, the **His**-functionalized nucleoside surrogate could be incorporated into DNA oligonucleotides by automated solid-phase synthesis (Table S1†). For control experiments, phenylalanine-conjugated derivatives were also prepared (Fig. S1–S4†).

A **His** residue was incorporated at the center of a 13-mer oligonucleotide (ODN 1: 5′–GCATGGXCACGGT–3′, where X = **His**) *via* automated solid-phase synthesis. Complementary strands containing native nucleobases or **His** in the center (ODN 2(Y): 5′-ACCGTGYCCATGC-3′, where Y = A, T, G, C, and **His**) were also prepared (Table 1 and Table S2†). The thermal stability of **His**-containing DNA duplexes was investigated using a DNA duplex containing a **His**–nucleobase (A, T, G, or C) pair and a duplex containing a **His**–**His** pair in the absence and presence of Cu(II) ions. DNA duplexes containing a **His**–nucleobase pair showed lower melting temperatures (T_m), around 40 °C, than duplexes containing a native A–T or G–C pair (53 °C and 63 °C, respectively). The observed decline in Tm indicated that the threoninol-tethered **His** residue did not recognize or interact with natural nucleobases. In addition, the presence of Cu(II) ions did not increase the thermal stability of the DNA duplexes containing a **His**–nucleobase pair. Interestingly, DNA duplexes containing a threoninol-tethered **His**–**His** pair showed higher Tm values than the duplexes containing a **His**–nucleobase pair. Moreover, after addition of 1 equivalent (eq.) of Cu(II) ions, the Tm value of DNA duplexes containing a **His**–**His** pair increased, up to 52 °C. For neighboring bases, the DNA duplexes containing ODN 3/ODN 4 (–A–**His**–T–) generally showed lower Tm values than the DNA duplexes containing ODN 1/ODN 2 (–G–**His**–C–) regardless of complementary nucleobases (Fig. S5 and S6†). And the thermal stabilization effect caused by the addition of 1 equivalent Cu(II) ion on the **His**–**His** pair was observed, however, T_m value decreased by the equivalent of Cu(II) ions increased (Fig. S9†). The results from thermal denaturation experiments with **His**–**His** pair-containing DNA duplexes in the presence of Cu(II) ions encouraged us to investigate the metal-binding ability of **His**-modified DNA duplexes.

We performed Tm measurements with duplexes containing a **His**–**His** pair in the presence of various metal ions. Besides Cu(II) ion, the addition of 1 eq of Zn(II) and Ni(II) ions significantly increased Tm values of duplexes to 48.7 °C and 50.3 °C, respectively (Fig. S9–S11†). However, the addition of Fe(II) did not increase the Tm of the duplexes (Fig. S8†). Circular dichroism (CD) measurements showed that the addition of 1 eq. of metal ions did not change the global structures of duplexes as a characteristic feature of typical right-handed B-DNA (Fig. S21–S26†).

Table 1 Sequences of oligonucleotides used in this study

Name	DNA sequences
ODN 1	5′-GCATGG-**His**-CACGGT-3′
ODN 2 (Y)	5′-ACCGTG-**Y**-CCATGC-3′ (Y = A, T, G, C, and **His**)
ODN 3	5′-GCATGA-**His**-TACGGT-3′
ODN 4 (Y)	5′-ACCGTA-**Y**-TCATGC-3′ (Y = A, T, G, C, and **His**)
ODN 5	5′-GCATGG-**His**-**His**-CACGGT-3′
ODN 6	5′-ACCGTG-**His**-**His**-CCATGC-3′
ODN 7	5′-GCATGA-**His**-**His**-TACGGT-3′
ODN 8	5′-ACCGTA-**His**-**His**-TCATGC-3′
ODN 9	5′-**GG**-**His**-**His**-**GG**-3′
ODN 10	5′-**GG**-**His**-**His**-**GG** CGCGAAG-3′
ODN 11	5′-CTTCGCG **GG**-**His**-**His**-**GG**-3′
ODN 12	5′-**GG**-**Ala**-**His**-**GG** CGCGAAG-3′
ODN 13	5′-CTTCGCG **GG**-**Ala**-**His**-**GG**-3′
ODN 14	5′-GCATGG-A-T-CACGGT-3′
ODN 15	5′-ACCGTG-A-T-CCATGC-3′
ODN 16	5′-**GG**-T-T-**GG** CGCGAAG-3′
ODN 17	5′-CTTCGCG **GG**-T-T-**GG**-3′

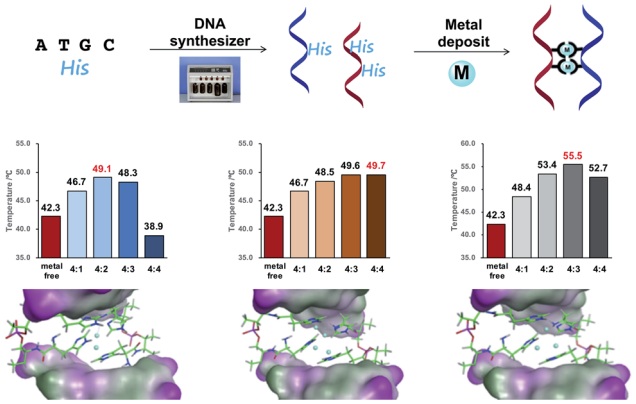

Fig. 1 Thermal stability assay and the plausible metal-deposit model of ODN 5/ODN 6 in the presence of various equivalent of metal ions. (A) The generation of a library of the histidine-conjugated DNA oligomers and the metal-deposit ability of the modified DNA, (B) thermal stability assay of ODN 5/ODN 6 in the presence of various equivalent of metal ions (The ratio on *x*-axial indicates histidine residue- : equivalent of metal ion).

Subsequently, as shown in Fig. 1A, we prepared DNA oligonucleotides with two consecutive **His** residues incorporated at the center of the DNA strands and investigated their metal-binding ability using thermal denaturation experiments according to the equivalence ratio of metal ion and DNA (Fig. 1B). DNA duplexes ODN 5/ODN 6 have a metal-binding site that consists of four **His** residues. We changed the molar ratio of metal ions to DNA duplex from 1 : 1 to 4 : 1 and found that T_m varied depending on the equivalence ratio as well as the type of metal ions (Fig. S13–S16†). For instance, the highest T_m was observed with 2 eq. of Cu(II) ions, 3 or 4 eq. of Zn(II) ions, and 3 eq. of Ni(II) ions. This indicated distinct thermal stabilization effects according to the metal ions used. Regardless of the molar ratio of metal ions to DNA duplex, Ni(II) ions led to the highest T_m value in all cases. No thermal stabilization compared with metal-free conditions was observed by the addition of iron ions (Fig. S13†).

To verify the thermal stabilization induced by metal-**His** binding, the **His** residue was replaced with phenylalanine residues, which are incapable of coordinating to the metal ions. In control experiments with DNA duplexes containing phenylalanine pairs, the thermal stability of the DNA duplexes changed only marginally in the presence of all examined metal ions, indicating that the observed thermal stabilization effects are caused by the metal-binding **His** residue. To rule out the thermal stabilization effect caused by the interaction between metal ions and the anionic phosphate backbone, we performed thermal denaturation experiments with native DNA duplexes (ODN 14/ODN 15) in the presence of various metal ions. No increase in T_m was observed even if up to 4 eq. of metal ions (copper, zinc, and nickel) were added to the DNA (Fig. S7†). These results support the hypothesis that the increase in T_m of the duplexes is attributed to the binding of metal ions to **His** residues and clearly indicate the potential of the **His**–DNA hybrid as a molecular reservoir for metal ions.

Besides the canonical Watson–Crick duplex, there are various noncanonical secondary structures, such as left-handed Z-DNA, triplex, and quadruplexes, under specific conditions.[42–45] Among them, G-quadruplex has been actively explored as a versatile scaffold for the construction of nanostructures because of its structural diversity, which is derived from combinations of parallel and antiparallel strands, different loop sequences, and shapes.[46–48] In this context, we incorporated **His** residues into a G-rich oligonucleotide, 5′-GG–**His**–**His**–GG-3′ (ODN 9), to construct a minimal G-quadruplex structure and investigated its conformational properties and metal-binding ability.[49] In the presence of K^+ ions, the CD spectra of ODN 9 indicated that the **His**-functionalized oligonucleotide forms a G-quadruplex structure with parallel conformation (Fig. 2B). We then also investigated the conformational changes induced by various other metal ions (Fig. 2A). On the addition of Cu(II) ions, ODN 9 showed a parallel conformation similar to that under metal-free conditions. In contrast, the addition of Co(II) ions induced antiparallel conformations. An antiparallel conformation was also observed in the presence of Ni(II) ions. On the addition of Zn(II) ions, the CD spectra of ODN 9 indicated hybrid or mixed conformations. Interestingly, the **His**-modified minimal G-quadruplex-forming sequence ODN 9 showed various topologies induced by metal complexations. This result indicated that the **His**-modified DNA nucleotides could be versatile building blocks for creating metal-triggered switchable nanostructures as well as biomolecular depots for metal ions.

Next, we investigated the utility of DNA duplexes involving threoninol-tethered **His** residues. DNA-based hybrid catalysts are one of the promising alternatives to develop water-compatible catalysts. Due to thermal and chemical stability, conformational flexibility, and automated solid-phase synthesis procedure, DNA has been actively explored as a biomolecular scaffold for catalysis.[50–52] In this study, the well-established asymmetric Diels–Alder reaction between aza-chalcone and cyclopentadiene was selected as a model reaction to investigate the performance of **His**-conjugated DNA as an asymmetric

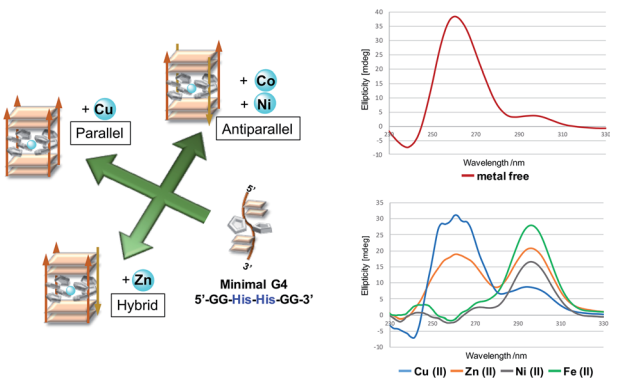

Fig. 2 CD spectra of ODN 9 in the presence of various metal ions. (A) Conceptual illustration for transformational conformations of ODN 9 in the presence of 1 equivalent of various metal ions, (B) CD spectra of ODN 9 in the absence and in the presence of 1 equivalent of metal ions.

Table 2 Asymmetric Diels–Alder reaction catalyzed by histidine-conjugated DNA-based hybrid catalysts containing Cu(II)[a]

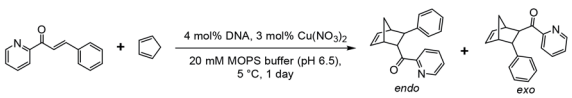

Entry[a]	DNA sequences	ee (%)	*endo*/*exo*	Conv. (%)
1	**His** monomer	+10	5/1	13
2	5′-GCATGG-**His**-CACGGT-3′ (**ODN 1**) 3′-CGTACC-**His**-GTGCCA-5′ (**ODN 2 (His)**)	+62	34/1	13
3	5′-GCATGA-**His**-TACGGT-3′ (**ODN 3**) 3′-CGTACT-**His**-ATGCCA-5′ (**ODN 4 (His)**)	+55	27/1	60
4	5′-GCATGG-**His**-**His**-CACGGT-3′ (**ODN 5**) 3′-CGTACC-**His**-**His**-GTGCCA-5′ (**ODN 6**)	+97	96/1	24
5	5′-GCATGA-**His**-**His**-TACGGT-3′ (**ODN 7**) 3′-CGTACT-**His**-**His**-ATGCCA-5′ (**ODN 8**)	**+95**	**59/1**	**90**

[a] Experiments were carried out using 3.3 mM aza-chalcone, 80 mM cyclopentadiene, 0.13 mM DNA, and 0.1 mM $Cu(NO_3)_2$ at 5 °C in 20 mM MOPS buffer (pH 6.5) for 1 day. The conversion and enantioselectivities were determined by chiral HPLC analysis.

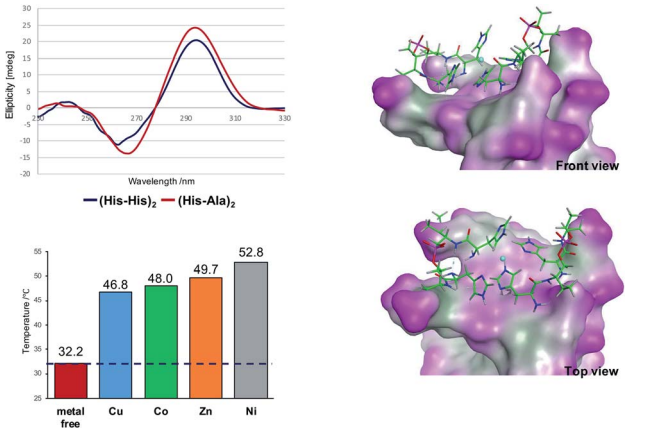

Fig. 3 Spectroscopic studies and the plausible model of ODN 10/ODN 11 and ODN 12/ODN 13 in the presence of various metal ions. (A) CD spectra of ODN 10/ODN11 and ODN 12/ODN 13 in the absence of metal ion, (B) thermal stability assay of ODN 10/ODN11 and ODN 12/ODN 13, (C) the plausible metal-coordinated molecular modeling model of ODN 10/ODN11 and ODN 12/ODN 13 in the presence of 1 equivalent of metal ions.

catalyst. While a control experiment using Cu(II) ions and **His**-conjugated D-threoninol monomer resulted in low *endo*/*exo* selectivity and enantioselectivity (Table 2, entry 1), in the presence of Cu(II) ions, the DNA duplex containing a D-threoninol-tethered **His**–**His** pair showed significantly increased enantioselectivity as well as *endo*/*exo* selectivity, indicating the potential of the DNA scaffold to induce high enantioselectivity (Table 2, entries 2 and 3). Under optimized conditions, Cu(II)/DNA duplex with four **His** residues resulted in the corresponding product with high conversion (90%), high *endo*/*exo* selectivity, and excellent enantioselectivity (+95% ee, Table 2, entry 5).

Moreover, we explored the usability of the **His**-modified G-quadruplex DNA in catalysis. It has been reported that the hemin/G-quadruplex DNA complex promotes the H_2O_2-mediated oxidation of ABTS to form colorimetric products from $ABTS^{2-}$.[53,54] The ABTS oxidation assay is a useful chromophore-based tool for quantifying oxidative catalytic ability. We evaluated the catalytic performance of the **His**-modified G-quadruplex DNA with hemin complex based on readout the corresponding radical species in ABTS oxidation reaction.

In this experiment, we designed the **His**-modified DNA quadruplex–duplex hybrid to focus on the effect of **His** residue on the well-organized strand topology of DNA. Based on the compatibility of quadruplex and duplex DNAs and their modulated topologies reported by Phan and colleagues,[55–57] two stacks of G-tetrad core with four **His** residues were elongated with duplex-forming sequences (ODN 10/ODN 11). DNA quadruplex–duplex hybrids with two histidine and two alanine residues were also prepared in the same manner (ODN 12/ODN 13). In the presence of K^+ ions, ODN 10/ODN 11 and ODN 12/ODN 13 formed antiparallel conformations, as confirmed by CD spectroscopy (Fig. 3A, S32 and S33†). The DNA quadruplex–duplex hybrid with four modified **His** residues showed a remarkable thermal stabilization effect in the presence of various metal ions, indicating a high storage capacity for metal ions (Fig. 3B, S17 and S18†). Unlike minimal G-quadruplex DNA (5′-GG–**His**–**His**–GG-3′, ODN 9), for the **His**-modified DNA quadruplex–duplex hybrids, we observed consistent antiparallel conformations in the presence of potassium and various other metal ions.

The **His**-modified DNA quadruplex–duplex hybrids with hemin were examined in the ABTS oxidation assay, and the initial rates (V_o) were determined to quantify the catalytic performance (Fig. 4, S37 and S38†). We found that hemin/quadruplex–duplex hybrids containing **His** residues catalyzed the ABTS oxidation reaction. Generally, in ABTS oxidation reactions, parallel conformations of G-quadruplex tend to have higher activities than antiparallel conformations.[58,59] Surprisingly, our **His**-modified DNA quadruplex–duplex hybrids with hemin efficiently promoted ABTS oxidation reaction despite their antiparallel conformations. The effectiveness of the **His** modification was evident compared with unmodified DNA quadruplex–duplex hybrid (ODN 16/ODN 17) in the control experiment. In the native

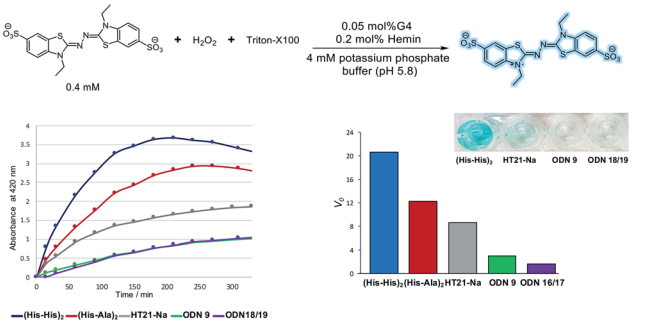

Fig. 4 ABTS oxidative reaction catalyzed by histidine-conjugated quadruplex–duplex hybrids. (A) The absorbance profiling graph of ABTS oxidation reaction catalyzed by various quadruplex forming DNA oligomers (profiling at 420 nm), (B) the comparison of the initial rate (V_o) and the image of ABTS oxidation reactions (15 min after adding H_2O_2).

horseradish peroxidase enzymes, a **His** residue binds to the hemin iron atom and promotes the oxidation reaction.[60–62] Our results indicated that the catalytic ability of unconventional antiparallel-based DNAzymes could be enhanced by a direct incorporation of **His** residue into the DNA scaffold.

Conclusions

In this study, we incorporated **His**, a representative metal-binding amino acid residue, into DNA oligonucleotides *via* an acyclic D-threoninol backbone. **His**-modified DNA duplexes showed remarkable metal-binding ability depending on the type of metal ion and the secondary structures of DNA. Furthermore, **His**-modified DNA oligonucleotides could be successfully used in DNA-based asymmetric catalysis as well as ABTS oxidation reactions. This will find important applications as an attractive approach to construct fine-tuned coordination environment for the biomimetic system of multimetal enzymes and the alternative of bioremediation. It is noteworthy that the present approach is as applicable to any other amino acid as to **His**. The present study is significant as it provides new insights into the incorporation of amino acid residues into nucleic acid scaffolds. Furthermore, we have also synthesized phenylalanine, alanine, and lysine-modified DNA oligonucleotides for conducting experiments comparable with those in this study (Fig. S2–S4, S19, S20, S34 and S35†). Research related to the development of new hybrid biomolecular systems by combining amino acids and nucleic acids is already under way.

Conflicts of interest

There are no conflicts to declare.

Acknowledgements

We express sincere thanks for a Grant-in-Aid Priority Research (16H06356 for H. S) from Japan Society for the Promotion of Science (JSPS). We also thank KAKENHI program (Grant-in-Aid for scientific research C, 18K05315) for support to S. P. We like to thank Karin Nishimura (Graduate School of Engineering, Kyoto University) for technical assistance to measure mass spectra of synthetic compounds.

Notes and references

1 P. H. von Hippel and O. G. Berg, *Proc. Natl. Acad. Sci. U. S. A.*, 1986, **83**, 1608.
2 S. L. Beaucage and R. P. Iyer, *Tetrahedron*, 1992, **48**, 2223.
3 N. C. Seeman, *Nature*, 2003, **421**, 427.
4 L. Pray, *Nature Education*, 2008, **1**, 100.
5 P. W. Rothemund, *Nature*, 2006, **440**, 297.
6 J. Bath and A. J. Turberfield, *Nat. Nanotechnol.*, 2007, **2**, 275.
7 J. L. Mergny and D. Sen, *Chem. Rev.*, 2019, **119**, 6290.
8 H. S. Rye, S. Yue, D. E. Wemmer, M. A. Quesada, R. P. Haugland, R. A. Mathies and A. N. Glazer, *Nucleic Acids Res.*, 1992, **20**, 2803.
9 J. Ju, C. Ruan, C. W. Fuller, A. N. Glazer and R. A. Mathies, *Proc. Natl. Acad. Sci. U. S. A.*, 1995, **92**, 4347.
10 C. T. Wittwer, M. G. Herrmann, A. A. Moss and R. P. Rasmussen, *Biotechniques*, 1997, **22**, 130.
11 S. T. Crooke, *FASEB J.*, 1993, **7**, 533.
12 S. T. Crooke and B. Lebleu, *Antisense research and applications*, 1993, CRC press.
13 L. H. Hurley, *Nat. Rev. Cancer*, 2002, **2**, 188.
14 D. R. A. J. L. B. L. Magda, R. A. Miller, J. L. Sessler and B. L. Iverson, *J. Am. Chem. Soc.*, 1994, **116**, 7439.
15 N. S. Oltra and G. Roelfes, *Chem. Commun.*, 2008, **45**, 6039.
16 P. Fournier, R. Fiammengo and A. Jäschke, *Angew. Chem., Int. Ed.*, 2009, **48**, 4426.
17 K. Tanaka, A. Tengeiji, T. Kato, N. Toyama and M. Shionoya, *Science*, 2003, **299**, 1212.
18 E. Meggers, P. L. Holland, W. B. Tolman, F. E. Romesberg and P. G. Schultz, *J. Am. Chem. Soc.*, 2000, **122**, 10714.
19 H. Weizman and Y. Tor, *J. Am. Chem. Soc.*, 2001, **123**, 3375.
20 C. J. Murphy, M. R. Arkin, Y. Jenkins, N. D. Ghatlia, S. H. Bossmann, N. J. Turro and J. K. Barton, *Science*, 1993, **262**, 1025.
21 T. J. Meade and J. F. Kayyem, *Angew. Chem., Int. Ed.*, 1995, **34**, 352.
22 O. I. Wilner and I. Willner, *Chem. Rev.*, 2012, **112**, 2528.
23 J. Bos and G. Roelfes, *Curr. Opin. Chem. Biol.*, 2014, **19**, 135.
24 S. Park, I. Okamura, S. Sakashita, J. H. Yum, C. Acharya, L. Gao and H. Sugiyama, *ACS Catal.*, 2015, **5**, 4708.
25 S. Dey, C. L. Rühl and A. Jäschke, *Chem.–Eur. J.*, 2017, **23**, 12162.
26 J. Mansot, S. Aubert, N. Duchemin, J. J. Vasseur, S. Arseniyadis and M. Smietana, *Chem. Sci.*, 2019, **10**, 2875.
27 H. A. Wagenknecht, *Angew. Chem., Int. Ed.*, 2003, **42**, 3204.
28 S. Park, L. Zheng, S. Kumakiri, S. Sakashita, H. Otomo, K. Ikehata and H. Sugiyama, *ACS Catal.*, 2014, **4**, 4070.
29 E. Golub, H. B. Albada, W. C. Liao, Y. Biniuri and I. Willner, *J. Am. Chem. Soc.*, 2015, **138**, 164.
30 S. Park and H. Sugiyama, *Angew. Chem., Int. Ed.*, 2010, **49**, 3870.
31 S. Park and H. Sugiyama, *Molecules*, 2012, **17**, 12792.
32 J. H. Yum, S. Park and H. Sugiyama, *Org. Biomol. Chem.*, 2019, **17**, 9547.
33 J. H. Yum, S. Park, R. Hiraga, I. Okamura, S. Notsu, S. Park and H. Sugiyama, *Org. Biomol. Chem.*, 2019, **17**, 2548.
34 S. Johannsen, N. Megger, D. Böhme, R. K. Sigel and J. Müller, *Nat. Chem.*, 2010, **2**, 229.
35 P. Scharf and J. Müller, *ChemPlusChem*, 2013, **78**, 20.
36 K. Schweizer, J. Kösters and J. Müller, *J. Biol. Inorg Chem.*, 2015, **20**, 895.
37 P. M. Punt and G. H. Clever, *Chem. Sci.*, 2019, **10**, 2513.
38 P. M. Punt and G. H. Clever, *Chem.–Eur. J.*, 2019, **25**, 13987.
39 H. Kashida, K. Sekiguchi, X. Liang and H. Asanuma, *J. Am. Chem. Soc.*, 2010, **132**, 6223.
40 H. Kashida, K. Murayama, T. Toda and H. Asanuma, *Angew. Chem., Int. Ed.*, 2011, **50**, 1285.
41 K. Murayama, Y. Tanaka, T. Toda, H. Kashida and H. Asanuma, *Chem.–Eur. J.*, 2013, **19**, 14151.

42 G. Gupta, M. Bansal and V. Sasisekharan, *Proc. Natl. Acad. Sci. U. S. A.*, 1980, **77**, 6486.
43 R. D. Wells, D. A. Collier, J. C. Hanvey, M. Shimizu and F. Wohlrab, *FASEB J.*, 1988, **2**, 2939.
44 A. T. Phan, V. Kuryavyi and D. J. Patel, *Curr. Opin. Struct. Biol.*, 2006, **16**, 288.
45 J. Choi and T. Majima, *Chem. Soc. Rev.*, 2011, **40**, 5893.
46 S. Burge, G. N. Parkinson, P. Hazel, A. K. Todd and S. Neidle, *Nucleic Acids Res.*, 2006, **34**, 5402.
47 A. T. Phan, V. Kuryavyi, K. N. Luu and D. J. Patel, *Quadruplex Nucleic Acids*, 2006, **7**, 81.
48 J. L. Huppert, *FEBS J.*, 2010, **277**, 3452.
49 J. Thevarpadam, I. Bessi, O. Binas, D. P. Gonçalves, C. Slavov, H. R. Jonker, C. Richter, J. Wachtveitl, H. Schwalbe and A. Heckel, *Angew. Chem., Int. Ed.*, 2016, **55**, 2738.
50 D. A. Baum and S. K. Silverman, *Cell. Mol. Life Sci.*, 2008, **65**, 2156.
51 A. J. Boersma, R. P. Megens, B. L. Feringa and G. Roelfes, *Chem. Soc. Rev.*, 2010, **39**, 2083.
52 N. Duchemin, I. Heath-Apostolopoulos, M. Smietana and S. Arseniyadis, *Org. Biomol. Chem.*, 2017, **15**, 7072.
53 P. Travascio, Y. Li and D. Sen, *Chem. Biol.*, 1998, **5**, 505.
54 P. Travascio, A. J. Bennet, D. Y. Wang and D. Sen, *Chem. Biol.*, 1999, **6**, 779.
55 K. W. Lim, Z. J. Khong and A. T. Phan, *Biochemistry*, 2013, **53**, 247.
56 K. W. Lim and A. T. Phan, *Angew. Chem., Int. Ed.*, 2013, **52**, 8566.
57 K. W. Lim, T. Q. N. Nguyen and A. T. Phan, *J. Am. Chem. Soc.*, 2014, **136**, 17969.
58 X. Cheng, X. Liu, T. Bing, Z. Cao and D. Shangguan, *Biochemistry*, 2009, **48**, 7817.
59 D. M. Kong, W. Yang, J. Wu, C. X. Li and H. X. Shen, *Analyst*, 2010, **135**, 321.
60 T. L. Poulos and J. Kraut, *J. Biol. Chem.*, 1980, **255**, 8199.
61 R. A. Marcus and N. Sutin, *Biochim. Biophys. Acta, Rev. Bioenerg.*, 1985, **811**, 265.
62 J. H. Dawson, *Science*, 1988, **240**, 433.